Springer

KSME

Journal of Mechanical Science and Technology 33 (6) (2019) 2903~2914
www.springerlink.com/content/1738-494x(Print)/1976-3824(Online)
DOI 10.1007/s12206-019-0538-0

On the fuzzy-adaptive command filtered backstepping control of an underactuated autonomous underwater vehicle in the three-dimensional space †

JinQiang Wang, Cong Wang*, YingJie Wei and ChengJu Zhang

School of Astronautics, Harbin Institute of Technology, Harbin, 150001, China

(Manuscript Received September 6, 2018; Revised February 12, 2019; Accepted March 5, 2019)

Abstract

This paper studies the three-dimensional path following control problem for an underactuated autonomous underwater vehicle in the presence of parameter uncertainties and external disturbances. Firstly, an appropriate model for the error dynamics was established to solve the path following problem in a moving Serret-Frenet frame. Secondly, an adaptive robust control scheme is proposed through fuzzy logic theory, command filtered backstepping method and an adaptation mechanism. Finally, a suitable Lyapunov candidate function is utilized to verify the stability of the overall control system and demonstrate uniform ultimate boundedness of path following errors. Following novelties are highlighted in this study: (i) The fuzzy method is adopted to solve the problems of model uncertainties, which makes the controller more practical; (ii) to calculate the virtual control derivative, a second-order filter is designed. This reduces the computational effort of the standard backstepping technique. Moreover, the effect of high frequency measurement noise is considerably attenuated via an appropriate filter to attain a more robust control system. (iii) To attain a desired approximation accuracy between the virtual control and the filtered signals, a compensation loop containing the filtered error is established. (iv) An anti-windup design is proposed to solve the problem of integral saturation in control input signals. Finally, comparative simulations are performed to ensure that the presented control scheme has excellent following accuracy and good robustness under multiple uncertainties and external disturbances.

Keywords: Underactuated underwater vehicle; Path following control; Backstepping; Fuzzy logic; Multiple uncertainties

1. Introduction

In the past several decades, a new underwater robotic system, called as the autonomous underwater vehicle (AUV) plays a significant role in the applications of ocean resource and military affairs, for instance, geomorphologic mapping, 3D seafloor imaging, ocean environment detection, deep sea archaeology, marine biology, pipeline inspection, oil and gas industry [1-5]. Different underwater goals could be realized using the path following control of AUV [6]. However, most of AUVs are underactuated, which means that they have a lower number of independent control inputs than the predefined degrees of freedom (DOF) that should be controlled. The lack of control inputs in sway and heave actuation presents a great challenge for designing the path following controllers due to the underactuated configurations such as nonholonomic, extremely nonlinear, time-varying, and powerful coupling between the motions of six DOF [7]. Furthermore, the model parameters of AUVs are greatly difficult to be accurately obtained, and their motions are strongly affected by environmental disturbances including the ocean currents, waves and so on. In this sense, the path following control of underactuated AUVs has become one of the most complicated problems in the robotic area.

Recently, many scholars have begun to pay attention to the path following control problems, and much of the work has been addressed in several publications. Appropriate line-of-sight (LOS) guidance based methods are employed on the horizontal path following and further researches have been addressed in Refs. [8-11]. Moreover, the backstepping control technique is also very popular in path following control problem of the underactuated vehicles. In Refs. [12, 13], an adaptive backstepping controller with a Lyapunov based adaptation mechanism has been developed for horizontal tracking. In Ref. [14], to reduce the complexity of controller, a novel approach based on feedback gain backstepping and Lyapunov stability theory has been presented. In Ref. [15], to achieve global asymptotic stability of the path following error, a global path following approach for the underactuated AUVs based on the same coordinates was proposed. In Ref. [16], the virtual guidance method was employed to construct the path following error model and a path following control scheme was de-

*Corresponding author. Tel.: +86 86413510, Fax.: +86 86413510
E-mail address: alanwang@hit.edu.cn
† Recommended by Associate Editor Baek-Kyu Cho

signed in the presence of constant ocean current disturbances. However, the control scheme has a significant limitation that the initial following errors should be lower than the minimum radius of the desired path. In Ref. [17], the dynamic surface control (DSC) approach has been employed to design a controller and the neural network technique has been utilized to estimate and compensate model uncertainties and external disturbances of the underactuated AUVs. In Ref. [18], an adaptive backstepping control method based on the radial basis function neural networks (RBFNNs) has been presented to solve the path following problem of a marine surface vehicle (MSV) under multiple uncertainties and actuator saturation. Unfortunately, for the neural network technology, it needs to achieve weight adjustments via advanced off-line learning or online learning. The main difficulty in this system is to obtain the optimum weight variations from the control signal and system output plus the desired system path [19]. Moreover, achieving the controller stability is also great of challenge. However, fuzzy logic approach employs the human heuristic knowledge to overcome the aforementioned shortcomings and control the system in the presence of uncertainties. This makes it as an appropriate choice for artificial intelligent objectives and capabilities [20]. In Ref. [21], a fuzzy sliding mode controller has been presented for way-points following subject to ocean current disturbances. In Ref. [22], an adaptive fuzzy sliding mode control structure under the multiple uncertainties for horizontal path following of AUV has been proposed. In Ref. [23], a fuzzy tracking controller with a direct adaptation mechanism has been presented under unknown parameters and external disturbances. In addition, a robust adaptive online constructive fuzzy technique has been utilized to cope with the multiple uncertainties of the control system. Unfortunately, solving the mentioned problems only in the horizontal plane has been considered in the literature. Nevertheless, the path problems in the three-dimensional space are much more challenging due to complex dynamics of underactuated AUVs and more DOFs without control input, which makes the controller design greatly difficult. Therefore, solving the mentioned control problem has been studied in only limited studies. In Ref. [24], a nonlinear robust controller employing the Lyapunov direct approach and backstepping technique has been proposed to enforce an underactuated AUV to reach and track a desired path in a three-dimensional space. However, in the mentioned study, the model parameters are considered unchanged. This assumption could not be realized in the real applications. In Ref. [25], dynamic surface control and backstepping approaches have been utilized to present a predefined spatial path following control scheme. However, uncertainties in the system parameters and external disturbances were not taken into consideration, which significantly limits its application in practice. In Ref. [26], a nonlinear robust control strategy via a command filtered backstepping approach has been developed to reduce the computational complexities of the standard backstepping method. However, in the mentioned work, multiple uncertainties were not considered. To sum up, all of the controllers mentioned in the early work have at least one of the following deficiencies. (i) In most of the early papers, the path following problems have been investigated only on the horizontal plane, which are not effective in the three-dimensional space; (ii) most previous controllers usually assumed that the multiple uncertainties are not taken into consideration or linear-in-parameter (LIP), which significantly limits their practical applications; (iii) the computational effort of the standard backstepping method could be considered as the third drawback. Motivated by the above considerations, a fuzzy-adaptive command filtered backstepping controller is proposed in the current paper for the underactuated AUVs, which is not addressed in sufficiently in the early researches.

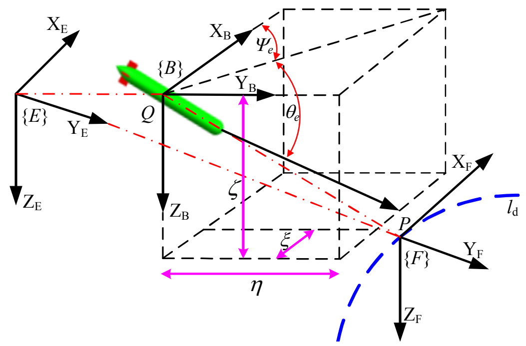

Fig. 1. The 3D AUV frames in the path following problem.

The rest of the current article is formed as follows. Sec. 2 introduces the AUV dynamics and problem formulation. The fuzzy-adaptive command filtered backstepping control strategy is developed in Sec. 3. The stability of the proposed control strategy is verified in Sec. 4. The simulation results compared with other methods are provided in Sec. 5. The obtained conclusions and future aspects are presented in Sec. 6.

2. AUV model and problem formulation

Fig. 1 illustrates the three-dimensional path following problem, where $\{E\},\{B\}$ and $\{SF\}$ represent the geodetic fixed frame, body fixed frame and the Serret-Frenet frame, respectively. l_d is the desired curvilinear path, which is independent with time. The origin of the $\{B\}$ frame coincides with the Q point, which is the AUV center of mass. The origin of $\{SF\}$ frame coincides with the P point which is the virtual reference guidance point on the desired path. Define ϖ is parameter of desired path, $[x_d(\varpi), y_d(\varpi), z_d(\varpi)]^{\mathrm{T}}$ is the position vector of Q in the Serret-Frenet frame, $[x, y, z]^{\mathrm{T}}$ is the coordinate vector of Q in the geodetic fixed frame, $[x_e, y_e, z_e]^{\mathrm{T}}$ and $[\xi, \eta, \zeta]^{\mathrm{T}}$ are the path following error vectors in the geodetic fixed frame and body fixed frame, respectively. Consider that the surge, sway, heave, pitch and yaw velocities of Q point in the body fixed frame are represented with u, v, w, q and r, respectively. We also define the course angles of the desired path as the following

$$\begin{cases} \theta_F = -\arctan\left(\dfrac{\dot{z}_d(\varpi)}{\sqrt{\dot{x}_d^2(\varpi)+\dot{y}_d^2(\varpi)}}\right) \\ \psi_F = \arctan\left(\dfrac{\dot{y}_d(\varpi)}{\dot{x}_d(\varpi)}\right) \end{cases} \tag{1}$$

where $\dot{x}_d = \dfrac{\partial x_d}{\partial \varpi}, \dot{y}_d = \dfrac{\partial y_d}{\partial \varpi}, \dot{z}_d = \dfrac{\partial z_d}{\partial \varpi}$, and the course angle errors are defined as ψ_e and θ_e, respectively.

2.1 The underactuated AUV model

The 3D dynamics of the AUV is proposed in this section. To reduce the overall complexity, we assume that the AUV rolling effects are neglected. Now, the 5DOF mathematical model of an underactuated AUV could be exploited as [27].

The AUV kinematic model is described as:

$$\begin{cases} \dot{x} = u\cos(\theta)\cos(\psi) - v\sin(\psi) + w\sin(\theta)\cos(\psi) \\ \dot{y} = u\cos(\theta)\sin(\psi) + v\cos(\psi) + w\sin(\theta)\sin(\psi) \\ \dot{z} = -u\sin(\theta) + w\cos(\theta) \\ \dot{\theta} = q \\ \dot{\psi} = r / \cos(\theta) . \end{cases} \tag{2}$$

The AUV dynamic model is described as:

$$\begin{cases} \dot{u} = \dfrac{m_{22}}{m_{11}}vr - \dfrac{m_{33}}{m_{11}}wq - \dfrac{f_u(u)}{m_{11}}u + \dfrac{\tau_u - \tau_{eu}(t)}{m_{11}} \\ \dot{v} = -\dfrac{m_{11}}{m_{22}}ur - \dfrac{f_v(v)}{m_{22}}v - \dfrac{1}{m_{22}}\tau_{ev}(t) \\ \dot{w} = \dfrac{m_{11}}{m_{33}}uq - \dfrac{f_w(w)}{m_{33}}w + \dfrac{1}{m_{33}}d_1 - \dfrac{1}{m_{33}}\tau_{ew}(t) \\ \dot{q} = \dfrac{m_{33}-m_{11}}{m_{55}}uw - \dfrac{f_q(q)}{m_{55}}q - \dfrac{1}{m_{55}}d_2 + \dfrac{\tau_q - \tau_{eq}(t)}{m_{55}} \\ \dot{r} = \dfrac{m_{11}-m_{22}}{m_{66}}uv - \dfrac{f_r(r)}{m_{66}}r + \dfrac{\tau_r - \tau_{er}(t)}{m_{66}} \end{cases} \tag{3}$$

where x, y, z, θ and ψ represent positions and orientations of the underactuated AUV in the geodetic fixed frame. Signals τ_u, τ_q and τ_r denote the control inputs which provided by the thrusters and propellers. $\tau_{eu}, \tau_{ev}, \tau_{ew}, \tau_{eq}$ and τ_{er} represent the bounded external disturbances induced by ocean currents, waves, and wind. $m_{ii}, i = 1,2,3,5,6$ denote the combined terms of mass and inertia parameters of AUV. $d_1 = (W - B)\cos\theta$, $d_2 = (z_g W - z_b B)\sin\theta$, where W and B denote the gravity and buoyancy of AUV. $f_k(k)$, $k = u, v, w, q, r$ stand for the AUV unknown hydrodynamic damping and friction terms, where $f_u(u) = X_u + X_{u|u|}|u|$, $f_v(v) = Y_v + Y_{v|v|}|v|$, $f_w(w) = Z_w + Z_{w|w|}|w|$ $f_q(q) = M_q + M_{q|q|}|q|$, $f_r(r) = N_r + N_{r|r|}|r|$. The rest signals and parameters are introduced in Ref. [28].

2.2 Error dynamics of the path following problem

To construct a control scheme for the path following problem, the system equations should be extracted in connection with the predefined path. According to Ref. [29], the path following dynamic error model of an underactuated AUV in the 3D space could be presented as follows:

$$\begin{cases} \dot{\xi} = r\xi - q\zeta + u - u_r\cos\theta_e\cos\psi_e \\ \dot{\eta} = -r\eta + v - u_r\cos\theta_e\sin\psi_e \\ \dot{\zeta} = q\xi + w + u_r\sin\theta_e . \end{cases} \tag{4}$$

The course angle error dynamic model is defined as:

$$\begin{cases} \dot{\theta}_e = q - \dot{\theta}_F \\ \dot{\psi}_e = r / \cos\theta - \dot{\psi}_F \end{cases} \tag{5}$$

where $\theta_e = \theta - \theta_F, \psi_e = \psi - \psi_F$, $\theta \in (-\pi/2, \pi/2)$, and u_r is velocity of the virtual reference guidance point.

3. Controller design

In this section, a 3D path following control structure is developed via the command filtered backstepping method, adaptive control techniques and fuzzy logic theory.

3.1 Position control of AUV

According to the Eq. (4), suppose the following Lyapunov function E as:

$$E = \frac{1}{2}\left(\xi^2 + \eta^2 + \zeta^2\right). \tag{6}$$

Differentiating Eq. (6) along with Eq. (4) yields:

$$\begin{aligned} \dot{E} &= \xi\dot{\xi} + \eta\dot{\eta} + \zeta\dot{\zeta} \\ &= \xi(u - u_r\cos\theta_e\cos\psi_e) + \zeta(w - u_r\sin\theta_e) \\ &\quad + \eta(v + u_r\cos\theta_e\sin\psi_e) . \end{aligned} \tag{7}$$

Then, we propose the following virtual control signals based on Eq. (7) as:

$$\begin{cases} u_c^0 = -k_1\xi + u_r\cos\theta_c^0\cos\psi_c^0 \\ \theta_c^0 = \arcsin\left(k_2\zeta / \sqrt{1+(k_2\zeta)^2}\right) \\ \psi_c^0 = -\arcsin\left(k_3\eta / \sqrt{1+(k_3\eta)^2}\right) \end{cases} \tag{8}$$

where $k_1 > 0, k_2 > 0, k_3 > 0$, and substituting Eq. (8) into Eq. (7) yields [30]:

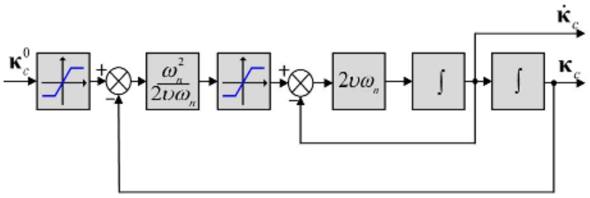

Fig. 2. Framework for a second-order filteter.

$$\dot{E} = -k_1\xi^2 + \eta v + \zeta w - k_2 u_r \frac{\zeta^2}{\sqrt{1+(k_2\zeta)^2}} - k_3 u_r \frac{\eta^2}{\sqrt{1+(k_3\eta)^2}} \frac{1}{\sqrt{1+(k_2\zeta)^2}} . \tag{9}$$

Then, to reduce the computational complexity in the standard backstepping control approach, the following second-order filter could be employed to calculate the derivatives of virtual control signals:

$$\ddot{\boldsymbol{\kappa}}_c = -2\upsilon\omega_n\dot{\boldsymbol{\kappa}}_c - \omega_n^2(\dot{\boldsymbol{\kappa}}_c - \boldsymbol{\kappa}_c^0) \tag{10}$$

where $\boldsymbol{\kappa}_c^0 = [\xi_c^0, \eta_c^0, \zeta_c^0, \theta_c^0, \psi_c^0, u_c^0, q_c^0, r_c^0]^{\mathrm{T}}$ is a vector including the desirable virtual control signals. $\boldsymbol{\kappa}_c = [\xi_c, \eta_c, \zeta_c, \theta_c, \psi_c, u_c, q_c, r_c]^{\mathrm{T}}$ is the vector of filtered signals, ω_n and υ are the parameters of the filter, where $0 < \omega_n < 1$ and $\upsilon > 0$. Fig. 2 describes the framework of the second-order filter.

Then, we consider the filtered path following errors as:

$$\begin{cases} \bar{\xi} = \xi - \xi_c \\ \bar{\eta} = \eta - \eta_c \\ \bar{\zeta} = \zeta - \zeta_c . \end{cases} \tag{11}$$

Differentiating Eq. (11) along with Eq. (4) yields:

$$\begin{bmatrix} \dot{\bar{\xi}} \\ \dot{\bar{\eta}} \\ \dot{\bar{\zeta}} \end{bmatrix} = \begin{bmatrix} r\bar{\eta} - q\bar{\zeta} \\ -r\bar{\xi} \\ q\bar{\xi} \end{bmatrix} + \begin{bmatrix} \mathbf{E} & \mathbf{M}\mathbf{g}(\bar{\psi})u_r & \mathbf{N}\mathbf{g}(\bar{\theta})u_r \end{bmatrix} \begin{bmatrix} \bar{u} \\ \bar{\psi} \\ \bar{\theta} \end{bmatrix} \tag{12}$$

where $\bar{u} = u - u_c, \bar{\psi} = \psi_e - \psi_c, \bar{\theta} = \theta_e - \theta_c$, $\mathbf{E} = [1,0,0]^{\mathrm{T}}$ and:

$$\mathbf{M} = \begin{bmatrix} \cos\theta_e\cos\psi_c & -\cos\theta_e\sin\psi_c \\ \cos\theta_c\sin\psi_c & \cos\theta_c\cos\psi_c \\ 0 & 0 \end{bmatrix} \quad \mathbf{g}(\bar{\psi}) = \begin{bmatrix} \dfrac{\cos\bar{\psi} - 1}{\bar{\psi}} \\ \dfrac{\sin\bar{\psi}}{\bar{\psi}} \end{bmatrix}$$

$$\mathbf{N} = \begin{bmatrix} \cos\theta_c\cos\psi_c & -\cos\psi_c\sin\theta_c \\ \cos\psi_e\cos\theta_c & -\sin\psi_e\sin\theta_c \\ -\sin\theta_c & -\cos\theta_c \end{bmatrix} \quad \mathbf{g}(\bar{\theta}) = \begin{bmatrix} \dfrac{\cos\bar{\theta} - 1}{\bar{\theta}} \\ \dfrac{\sin\bar{\theta}}{\bar{\theta}} \end{bmatrix}$$

where $\mathbf{g}(\bar{\psi})$ and $\mathbf{g}(\bar{\theta})$ satisfy:

$$\lim_{\bar{\psi}\to 0}\mathbf{g}(\bar{\psi}) = \begin{bmatrix} 0 \\ 1 \end{bmatrix}, \quad \lim_{\bar{\theta}\to 0}\mathbf{g}(\bar{\theta}) = \begin{bmatrix} 0 \\ 1 \end{bmatrix}.$$

Then, we construct the following position virtual control signals:

$$\begin{cases} \dot{\xi}_c^0 = -\alpha_\xi\bar{\xi} + \dot{\xi}_c \\ \dot{\eta}_c^0 = -\alpha_\eta\bar{\eta} + \dot{\eta}_c \\ \dot{\zeta}_c^0 = -\alpha_\zeta\bar{\zeta} + \dot{\zeta}_c . \end{cases} \tag{13}$$

Substitute Eq. (13) into Eq. (12), we get:

$$\begin{bmatrix} \dot{\bar{\xi}} \\ \dot{\bar{\eta}} \\ \dot{\bar{\zeta}} \end{bmatrix} = \begin{bmatrix} r\bar{\eta} - q\bar{\zeta} \\ -r\bar{\xi} \\ q\bar{\xi} \end{bmatrix} + \begin{bmatrix} -\alpha_\xi\bar{\xi} \\ -\alpha_\eta\bar{\eta} \\ -\alpha_\zeta\bar{\zeta} \end{bmatrix} + \begin{bmatrix} \dot{\xi}_c - \dot{\xi}_c^0 \\ \dot{\eta}_c - \dot{\eta}_c^0 \\ \dot{\zeta}_c - \dot{\zeta}_c^0 \end{bmatrix} + \begin{bmatrix} \mathbf{E} & \mathbf{M}\mathbf{g}(\bar{\psi})u_r & \mathbf{N}\mathbf{g}(\bar{\theta})u_r \end{bmatrix} \begin{bmatrix} \bar{u} \\ \bar{\psi} \\ \bar{\theta} \end{bmatrix} . \tag{14}$$

Then, to attain the desired approximation accuracy between the filtered signals and the command virtual control, the following position filtered error signals are defined as: $\chi_\xi = \bar{\xi} - \vartheta_\xi$, $\chi_\eta = \bar{\eta} - \vartheta_\eta$ and $\chi_\zeta = \bar{\zeta} - \vartheta_\zeta$, where $\vartheta_\xi, \vartheta_\eta$ and ϑ_ζ are defined as:

$$\begin{bmatrix} \dot{\vartheta}_\xi \\ \dot{\vartheta}_\eta \\ \dot{\vartheta}_\zeta \end{bmatrix} = \begin{bmatrix} r\vartheta_\eta - q\vartheta_\zeta \\ -r\vartheta_\xi \\ q\vartheta_\xi \end{bmatrix} + \begin{bmatrix} -\alpha_\xi\vartheta_\xi \\ -\alpha_\eta\vartheta_\eta \\ -\alpha_\zeta\vartheta_\zeta \end{bmatrix} + \begin{bmatrix} \dot{\xi}_c - \dot{\xi}_c^0 \\ \dot{\eta}_c - \dot{\eta}_c^0 \\ \dot{\zeta}_c - \dot{\zeta}_c^0 \end{bmatrix} + \begin{bmatrix} \mathbf{E} & \mathbf{M}\mathbf{g}(\bar{\psi})u_r & \mathbf{N}\mathbf{g}(\bar{\theta})u_r \end{bmatrix} \begin{bmatrix} \vartheta_u \\ \vartheta_\psi \\ \vartheta_\theta \end{bmatrix} \tag{15}$$

where $\vartheta_\xi(0) = 0, \vartheta_\eta(0) = 0$ and $\vartheta_\zeta(0) = 0$; ϑ_ψ and ϑ_θ are defined in Eq. (21). Now, assume the following Lyapunov candidate function:

$$E_1 = \frac{1}{2}\left(\chi_\xi^2 + \chi_\eta^2 + \chi_\zeta^2\right). \tag{16}$$

Differentiating Eq. (16) along with Eqs. (14) and (15), we get:

$$\dot{E}_1 = \chi_\xi\dot{\chi}_\xi + \chi_\eta\dot{\chi}_\eta + \chi_\zeta\dot{\chi}_\zeta = -\alpha_\xi\chi_\xi^2 - \alpha_\eta\chi_\eta^2 - \alpha_\zeta\chi_\zeta^2 + \left[\chi_\xi, \chi_\eta, \chi_\zeta\right] \times \begin{bmatrix} \mathbf{E} & \mathbf{M}\mathbf{g}(\bar{\psi})u_r & \mathbf{N}\mathbf{g}(\bar{\theta})u_r \end{bmatrix} \times \begin{bmatrix} \vartheta_u \\ \vartheta_\psi \\ \vartheta_\theta \end{bmatrix} \tag{17}$$

$$= -\alpha_\xi \chi_\xi^2 - \alpha_\eta \chi_\eta^2 - \alpha_\zeta \chi_\zeta^2 + \mathbf{E}^{\mathrm{T}}\left[\chi_\xi, \chi_\eta, \chi_\zeta\right]^{\mathrm{T}} \chi_u + \mathbf{g}(\overline{\psi})\mathbf{M}^{\mathrm{T}} \begin{bmatrix} \chi_\xi \\ \chi_\eta \\ \chi_\zeta \end{bmatrix} \chi_\psi u_r + \mathbf{g}(\overline{\theta})\mathbf{N}^{\mathrm{T}} \begin{bmatrix} \chi_\xi \\ \chi_\eta \\ \chi_\zeta \end{bmatrix} \chi_\theta u_r$$

where $\chi_u = \overline{u} = u - u_c$, $\chi_\psi = \overline{\psi} - \vartheta_\psi$ and $\chi_\theta = \overline{\theta} - \vartheta_\theta$.

3.2 Attitude control of AUV

Defining $\overline{\psi} = \psi_e - \psi_c, \overline{\theta} = \theta_e - \theta_c$, and differentiating $\overline{\psi}$ and $\overline{\theta}$ along with Eq. (5), we get:

$$\begin{cases} \dot{\overline{\psi}} = \dfrac{r}{\cos\theta} - r_F - \dot{\psi}_c = \dfrac{r_c^0 + (r_c - r_c^0) + \overline{r}}{\cos\theta} - r_F - \dot{\psi}_c \\ \dot{\overline{\theta}} = q - q_F - \dot{\theta}_c = q_c + (q_c - q_c^0) + \overline{q} - q_F - \dot{\theta}_c \end{cases} \tag{18}$$

where $\overline{r} = r - r_c, \overline{q} = q - q_c$. Then we consider the following desired virtual signals as:

$$\begin{cases} r_c^0 = \cos\theta(\dot{\psi}_c - \alpha_\psi \overline{\psi} - \psi_{bs} + r_F) \\ q_c^o = \dot{\theta}_c - \alpha_\theta \overline{\theta} - \theta_{bs} + q_F \end{cases} \tag{19}$$

where α_ψ and α_θ represent the arbitrary positive numbers. ψ_{bs} and θ_{bs} are the robust parts of the control system that will be defined in the next section. Then, replacement of Eq. (19) in Eq. (18) gives

$$\begin{cases} \dot{\overline{\psi}} = \dfrac{r_c^0 + (r_c - r_c^0) + \overline{r}}{\cos\theta} - \alpha_\psi \overline{\psi} - \psi_{bs} \\ \dot{\overline{\theta}} = (q_c - q_c^0) + \overline{q} - \alpha_\theta \overline{\theta} - \theta_{bs}. \end{cases} \tag{20}$$

Then, defining the following attitude filtered error signals as $\chi_\psi = \overline{\psi} - \vartheta_\psi$ and $\chi_\theta = \overline{\theta} - \vartheta_\theta$, where ϑ_ψ and ϑ_θ could be calculated as:

$$\begin{cases} \dot{\vartheta}_\psi = \dfrac{(r_c - r_c^0) + \vartheta_r}{\cos\theta} - \alpha_\psi \vartheta_\psi \\ \dot{\vartheta}_\theta = (q_c - q_c^0) + \vartheta_q - \alpha_\theta \vartheta_\theta \end{cases} \tag{21}$$

where $\vartheta_\psi(0) = 0$, $\vartheta_\theta(0) = 0$, $\vartheta_q = \vartheta_r = 0$. Now, the following Lyapunov candidate function could be defined

$$E_2 = \frac{1}{2}\left(\chi_\psi^2 + \chi_\theta^2\right). \tag{22}$$

Differentiating Eq. (22) along with Eqs. (20) and (21) yields:

$$\begin{aligned} \dot{E}_2 &= \chi_\psi \dot{\chi}_\psi + \chi_\theta \dot{\chi}_\theta \\ &= \left(\dot{\overline{\psi}} - \dot{\vartheta}_\psi\right)\chi_\psi + \left(\dot{\overline{\theta}} - \dot{\vartheta}_\theta\right)\chi_\theta \\ &= \left(\frac{\overline{r} - \vartheta_r}{\cos\theta} - \alpha_\psi \overline{\psi} - \psi_{bs} + \alpha_\psi \vartheta_\psi\right)\chi_\psi \\ &\quad + \left(-\alpha_\theta \overline{\theta} + \overline{q} - \theta_{bs} + \alpha_\theta \vartheta_\theta - \vartheta_q\right)\chi_\theta \\ &= -\alpha_\psi \chi_\psi^2 + \frac{\chi_r}{\cos\theta}\chi_\psi + \chi_q \chi_\theta - \theta_{bs}\chi_\theta - \psi_{bs}\chi_\psi - \alpha_\theta \chi_\theta^2 \end{aligned} \tag{23}$$

where $\chi_q = \overline{q} = q - q_c$ and $\chi_r = \overline{r} = r - r_c$.

3.3 Velocity control of AUV

We define $\dot{\overline{u}} = \dot{u} - \dot{u}_c, \dot{\overline{q}} = \dot{q} - \dot{q}_c, \dot{\overline{r}} = \dot{r} - \dot{r}_c$ and the following error equations could be proposed as

$$\begin{cases} m_{11}\dot{\overline{u}} = m_{22}vr - m_{33}wq - m_{11}\dot{u}_c - f_u(u)u + \tau_u - \tau_{eu}(t) \\ m_{55}\dot{\overline{q}} = (m_{33} - m_{11})uw - m_{55}\dot{q}_c - f_q(q)q - d_2 + \tau_q - \tau_{eq}(t) \\ m_{66}\dot{\overline{r}} = (m_{11} - m_{22})uv - m_{66}\dot{r}_c - f_r(r)r + \tau_r - \tau_{er}(t). \end{cases} \tag{24}$$

Then, the following controllers are presented:

$$\begin{cases} \tau_u = m_{11}(-\alpha_u \overline{u} + \dot{u}_c - u_{bs}) - m_{22}vr + m_{33}wq - f_u(u)u \\ \tau_q = m_{55}(-\alpha_q \overline{q} + \dot{q}_c - q_{bs}) - (m_{33} - m_{11})uw - f_q(q)q + d_2 \\ \tau_r = m_{66}(-\alpha_r \overline{r} + \dot{r}_c - r_{bs}) - (m_{11} - m_{22})uv - f_r(r)r \end{cases} \tag{25}$$

where α_u, α_q and α_r are the positive constants, u_{bs}, q_{bs} and r_{bs} are the system robust terms which will be designed in the next section.

In order to deal with the model uncertainties and external disturbances in the proposed control system, the fuzzy logic theory is utilized here. Suppose the following fuzzy logic rule:

R^j : if x_1 is A_1^j and x_2 is A_2^j and$\cdots$and
x_n is A_n^j, then $f(\mathbf{x})$ is B^j

where R^j denotes the fuzzy rules, $j = 1,2,3,....,k$. $f(\mathbf{x})$ is the system output; $\mathbf{x} = [x_1, x_2, x_3, ...x_n]^{\mathrm{T}}$ is control input vector. A_i^j and B^j represent fuzzy values that are represented with the membership function, and the average defuzzifier can be designed as [31]:

$$\hat{f}(\mathbf{x}|\boldsymbol{\theta}) = \sum_{j=1}^{k}\sigma_j(\mathbf{x})\theta_j = \hat{\boldsymbol{\theta}}^{\mathrm{T}}\boldsymbol{\sigma}(\mathbf{x}) \tag{26}$$

where $\boldsymbol{\theta} = [\theta_1, \theta_2, \theta_3, ..., \theta_k]^{\mathrm{T}}$ represents the vector of adaptation parameters. Moreover, the membership function $\sigma_j(\mathbf{x})$ is defined as

$$\sigma_j(\mathbf{x}) = \frac{\prod_{i=1}^{n=1}\mu_{Ai}^j(x_i)}{\sum_{j=1}^{k}\prod_{i=1}^{n=1}\mu_{Ai}^j(x_i)}. \tag{27}$$

We assume that $\mathbf{x}$ and $\boldsymbol{\theta}$ are parts of the compact sets

R and Ω. Now, the vector of optimal parameters could be defined as

$$\boldsymbol{\theta}^* = \arg\min_{\boldsymbol{\theta}\in\Omega}\left[\sup_{\mathbf{x}\in R}\left|\hat{f}(\mathbf{x}|\boldsymbol{\theta}) - f(\mathbf{x})\right|\right] \tag{28}$$

and we get:

$$f(\mathbf{x}) = \boldsymbol{\theta}^{*\mathrm{T}}\boldsymbol{\sigma}(\mathbf{x}) + \varepsilon(\mathbf{x}) \tag{29}$$

where $\varepsilon(\mathbf{x})$ is the approximation error for $\boldsymbol{\theta}\to\boldsymbol{\theta}^*$, and $|\varepsilon(\mathbf{x})| \le \varepsilon_N$, where ε_N is a unknown positive constant.

As a result, the controller in surge direction is rewritten as:

$$\begin{cases}\tau_u = \hat{\boldsymbol{\theta}}_u\boldsymbol{\sigma}(\mathbf{x}_u) - \hat{\eta}_u\tanh(\nu\hat{\eta}_u\bar{u}/\mu_u) - m_{11}\alpha_u\bar{u} - m_{11}u_{bs} \\ \dot{\hat{\boldsymbol{\theta}}}_u = -\gamma_{wu}\left(\bar{u}\boldsymbol{\sigma}^{\mathrm{T}}(\mathbf{x}_u) + \lambda_u\hat{\boldsymbol{\theta}}_u\right) \\ \dot{\hat{\eta}}_u = \gamma_{\eta u}\left(|\bar{u}| - \kappa_u\hat{\eta}_u + \kappa_u\eta_{u0}\right)\end{cases} \tag{30}$$

where $\alpha_u,\mu_u,\gamma_{wu},\lambda_u,\gamma_{\eta u},\kappa_u,\eta_{u0}$ are the positive design parameters, $\nu = e^{-(\nu+1)}, \nu = 0.2785$, $\mathbf{x}_u = [u,v,w,q,r,\dot{u}_c]^{\mathrm{T}}$ is the input vector of the fuzzy logic system, and the corresponding membership function is designed as:

$$\sigma_j^1(\mathbf{x}_u) = \exp\left[-\left(\left(\mathbf{x}_u + \frac{\rho_1}{8} - (j-1)\frac{\rho_1}{16}\right)/\sigma_1\right)^2\right] \tag{31}$$

where $j = 1,2,....,5$.

The controller in the pitch direction is rewritten as:

$$\begin{cases}\tau_q = \hat{\boldsymbol{\theta}}_q\boldsymbol{\sigma}(\mathbf{x}_q) - \hat{\eta}_q\tanh(\nu\hat{\eta}_q\bar{q}/\mu_q) - m_{55}\alpha_q\bar{q} - m_{55}q_{bs} \\ \dot{\hat{\boldsymbol{\theta}}}_q = -\gamma_{wq}\left(\bar{q}\boldsymbol{\sigma}^{\mathrm{T}}(\mathbf{x}_q) + \lambda_q\hat{\boldsymbol{\theta}}_q\right) \\ \dot{\hat{\eta}}_q = \gamma_{\eta q}\left(|\bar{q}| - \kappa_q\hat{\eta}_q + \kappa_q\eta_{q0}\right)\end{cases} \tag{32}$$

where $\alpha_q,\mu_q,\gamma_{wq},\lambda_q,\gamma_{\eta q},\kappa_q,\eta_{q0}$ are the positive design parameters, $\mathbf{x}_q = [u,w,q,\theta,\dot{q}_c]^{\mathrm{T}}$ is the input vector of the fuzzy logic system, and the corresponding membership function is designed as:

$$\sigma_j^2(\mathbf{x}_q) = \exp\left[-\left(\left(\mathbf{x}_q + \frac{\rho_2}{8} - (j-1)\frac{\rho_2}{16}\right)/\sigma_2\right)^2\right] \tag{33}$$

where $j = 1,2,....,5$.

In the yaw direction, the controller could be synthesized as

$$\begin{cases}\tau_r = \hat{\boldsymbol{\theta}}_r\boldsymbol{\sigma}(\mathbf{x}_r) - \hat{\eta}_r\tanh(\nu\hat{\eta}_r\bar{r}/\mu_r) - m_{66}\alpha_r\bar{r} - m_{66}r_{bs} \\ \dot{\hat{\boldsymbol{\theta}}}_r = -\gamma_{wr}\left(\bar{r}\boldsymbol{\sigma}^{\mathrm{T}}(\mathbf{x}_r) + \lambda_r\hat{\boldsymbol{\theta}}_r\right) \\ \dot{\hat{\eta}}_r = \gamma_{\eta r}\left(|\bar{r}| - \kappa_r\hat{\eta}_r + \kappa_r\eta_{r0}\right)\end{cases} \tag{34}$$

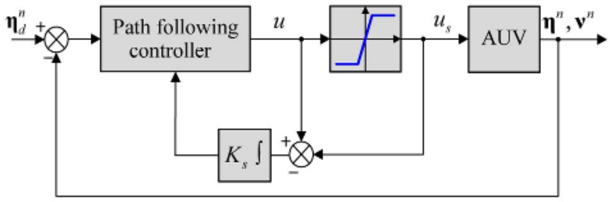

Fig. 3. The structure of anti-windup control part.

where $\alpha_r,\mu_r,\gamma_{wr},\lambda_r,\gamma_{\eta r},\kappa_r,\eta_{r0}$ are the positive design coefficients. $\mathbf{x}_r = [u,v,\mathrm{r},\dot{r}_c]^{\mathrm{T}}$ is the input vector of the fuzzy logic system, and the corresponding membership function is designed as:

$$\sigma_j^3(\mathbf{x}_r) = \exp\left[-\left(\left(\mathbf{x}_r + \frac{\rho_3}{8} - (j-1)\frac{\rho_3}{16}\right)/\sigma_3\right)^2\right] \tag{35}$$

where $j = 1,2,....,6$.

Then, substitute Eqs. (30), (32) and (34) into Eq. (25) and the system error dynamics is presented as follows:

$$\begin{cases}m_{11}\dot{\bar{u}} = -m_{11}(\alpha_u\bar{u} + u_{bs}) + \hat{\boldsymbol{\theta}}_u\boldsymbol{\sigma}(\mathbf{x}_u) - \hat{\eta}_u\tanh(\nu\hat{\eta}_u\bar{u}\mu_u^{-1}) - \xi_u \\ m_{55}\dot{\bar{q}} = -m_{55}(\alpha_q\bar{q} + q_{bs}) + \hat{\boldsymbol{\theta}}_q\boldsymbol{\sigma}(\mathbf{x}_q) - \hat{\eta}_q\tanh(\nu\hat{\eta}_q\bar{q}\mu_q^{-1}) - \xi_q \\ m_{66}\dot{\bar{r}} = -m_{66}(\alpha_r\bar{r} + r_{bs}) + \hat{\boldsymbol{\theta}}_r\boldsymbol{\sigma}(\mathbf{x}_r) - \hat{\eta}_r\tanh(\nu\hat{\eta}_r\bar{r}\mu_r^{-1}) - \xi_r\end{cases} \tag{36}$$

where ξ_u,ξ_q and ξ_r are given as

$$\begin{cases}\xi_u = -m_{22}vr + m_{33}wq + m_{11}\dot{u}_c + f_u(u)u + \tau_{eu}(t) \\ \xi_q = -(m_{33} - m_{11})uw + m_{55}\dot{q}_c + d_2 + f_q(q)q + \tau_{eq}(t) \\ \xi_r = -(m_{11} - m_{22})uv + m_{66}\dot{r}_c + f_r(r)r + \tau_{er}(t)\,.\end{cases} \tag{37}$$

3.4 Anti-windup design

To resolve the integral saturation problem in control input signals, an anti-windup design is proposed in this section. We define u is a control input signal, and u_s is a control input signal after the anti-windup design, which can be constructed as [26]:

$$u_s = \begin{cases}u_m, & u \ge u_m \\ u, & -u_m < u < u_m \\ u_m, & u \le -u_m\end{cases} \tag{38}$$

where u_m is limited amplitude of the control signal, and the controller of anti-windup part is designed as:

$$u = u_s - K_s\int(u - u_s)dt \tag{39}$$

where K_s is the positive gain parameter, and the structure of anti-windup part is shown as Fig. 3.

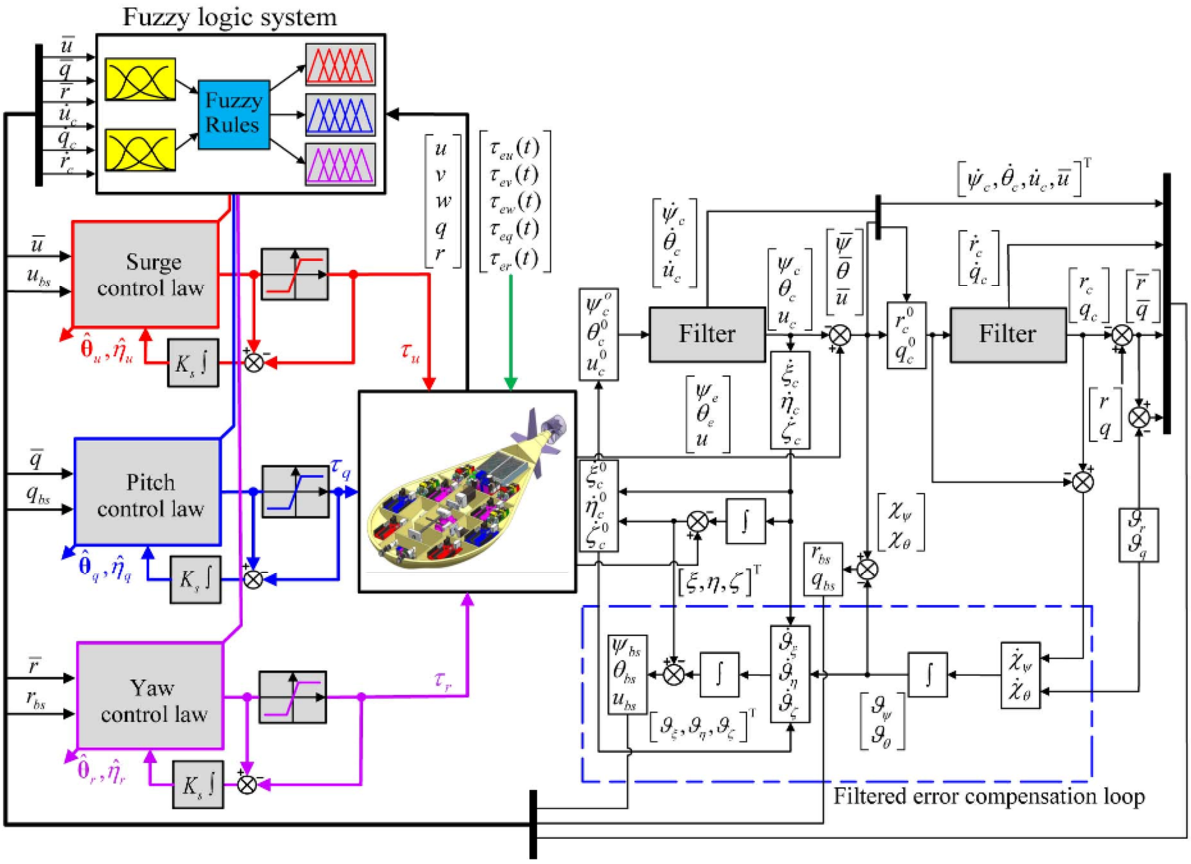

Fig. 4. The detailed block diagram of the proposed 3D path following control structure.

where $\boldsymbol{\eta}_d^n = [x_d(\varpi), y_d(\varpi), z_d(\varpi)]^{\mathrm{T}}$, $\mathbf{v}^n = [u, v, w, q, r]^{\mathrm{T}}$, and $\boldsymbol{\eta}^n = [\xi, \eta, \zeta]^{\mathrm{T}}$.

Fig. 4 gives a detailed block diagram of the presented 3D path following control structure for an underactuated AUV. In the upcoming section, the stability of the proposed control structure is studied.

4. Stability analysis of the overall control system

Theorem: Suppose that the kinematic and dynamic models of an underactuated AUV are described through Eqs. (2) and (3). The proposed fuzzy-adaptive command filtered backstepping controller Eqs. (30), (32) and (34) combined with the system robust terms Eqs. (42) and (43), gives the bounded signals for the overall control system. Moreover, the path following error signals uniformly tend to a narrow band around the origin.

Proof: Suppose the following Lyapunov candidate function for the overall control structure:

$$E_3 = \frac{1}{2}\left(\chi_\xi^2 + \chi_\eta^2 + \chi_\zeta^2 + \chi_\psi^2 + \chi_\theta^2 + m_{11}\bar{u}^2 + m_{55}\bar{q}^2 + m_{66}\bar{r}^2\right) + \frac{\bar{\boldsymbol{\theta}}_u^{\mathrm{T}}\bar{\boldsymbol{\theta}}_u}{2\gamma_{wu}} + \frac{\bar{\boldsymbol{\theta}}_q^{\mathrm{T}}\bar{\boldsymbol{\theta}}_q}{2\gamma_{wq}} + \frac{\bar{\boldsymbol{\theta}}_r^{\mathrm{T}}\bar{\boldsymbol{\theta}}_r}{2\gamma_{wr}} + \frac{\bar{\eta}_u^2}{2\gamma_{\eta u}} + \frac{\bar{\eta}_q^2}{2\gamma_{\eta q}} + \frac{\bar{\eta}_r^2}{2\gamma_{\eta r}} \tag{40}$$

where $\bar{\boldsymbol{\theta}}_k = \boldsymbol{\theta}_k^* - \hat{\boldsymbol{\theta}}_k$ and $\bar{\eta}_k = \eta_k^* - \hat{\eta}_k, k = u, q, r$ are weight and parameter estimation errors, respectively.

Then, differentiating Eq. (40) along with Eqs. (17), (23), (36) and (37) yields:

$$\begin{aligned}
\dot{E}_3 &= \chi_\xi\dot{\chi}_\xi + \chi_\eta\dot{\chi}_\eta + \chi_\zeta\dot{\chi}_\zeta + \chi_\psi\dot{\chi}_\psi + \chi_\theta\dot{\chi}_\theta + m_{11}\bar{u}\dot{\bar{u}} + m_{55}\bar{q}\dot{\bar{q}} \\
&\quad + m_{66}\bar{r}\dot{\bar{r}} - \bar{\boldsymbol{\theta}}_u^{\mathrm{T}}\gamma_{wu}^{-1}\dot{\hat{\boldsymbol{\theta}}}_u - \bar{\boldsymbol{\theta}}_q^{\mathrm{T}}\gamma_{wq}^{-1}\dot{\hat{\boldsymbol{\theta}}}_q - \bar{\boldsymbol{\theta}}_r^{\mathrm{T}}\gamma_{wr}^{-1}\dot{\hat{\boldsymbol{\theta}}}_r - \bar{\eta}_u\gamma_{\eta u}^{-1}\dot{\hat{\eta}}_u \\
&\quad - \bar{\eta}_q\gamma_{\eta q}^{-1}\dot{\hat{\eta}}_q - \bar{\eta}_r\gamma_{\eta r}^{-1}\dot{\hat{\eta}}_r \\
&= -\alpha_\xi\chi_\xi^2 - \alpha_\eta\chi_\eta^2 - \alpha_\zeta\chi_\zeta^2 - \alpha_\psi\chi_\psi^2 - \alpha_\theta\chi_\theta^2 - \alpha_u\bar{u}^2 - \alpha_q\bar{q}^2 - \alpha_r\bar{r}^2 \\
&\quad + \mathbf{E}^{\mathrm{T}}\begin{bmatrix}\chi_\xi \\ \chi_\eta \\ \chi_\zeta\end{bmatrix}\chi_u + \mathbf{g}^{\mathrm{T}}(\bar{\psi})\mathbf{M}^{\mathrm{T}}\begin{bmatrix}\chi_\xi \\ \chi_\eta \\ \chi_\zeta\end{bmatrix}\chi_\psi u_r + \mathbf{g}^{\mathrm{T}}(\bar{\theta})\mathbf{N}^{\mathrm{T}}\begin{bmatrix}\chi_\xi \\ \chi_\eta \\ \chi_\zeta\end{bmatrix}\chi_\theta u_r \\
&\quad + \frac{\chi_r}{\cos\theta}\chi_\psi - \theta_{bs}\chi_\theta + \chi_q\chi_\theta - \chi_q q_{bs} - \psi_{bs}\chi_\psi - \chi_r r_{bs} \\
&\quad - \chi_u u_{bs} - \chi_u\left(\bar{\boldsymbol{\theta}}_u\boldsymbol{\xi}(\mathbf{x}_u) + \hat{\eta}_u\tanh(\nu\hat{\eta}_u\bar{u}\mu_u^{-1}) + \varepsilon_u + \tau_{eu}(t)\right) \\
&\quad - \chi_q\left(\bar{\boldsymbol{\theta}}_q\boldsymbol{\xi}(\mathbf{x}_q) + \hat{\eta}_q\tanh(\nu\hat{\eta}_q\bar{q}\mu_q^{-1}) + \varepsilon_q + \tau_{eq}(t)\right) \\
&\quad - \chi_r\left(\bar{\boldsymbol{\theta}}_r\boldsymbol{\xi}(\mathbf{x}_r) + \hat{\eta}_r\tanh(\nu\hat{\eta}_r\bar{r}\mu_r^{-1}) + \varepsilon_r + \tau_{er}(t)\right) - \bar{\boldsymbol{\theta}}_u^{\mathrm{T}}\gamma_{wu}^{-1}\dot{\hat{\boldsymbol{\theta}}}_u \\
&\quad - \bar{\boldsymbol{\theta}}_q^{\mathrm{T}}\gamma_{wq}^{-1}\dot{\hat{\boldsymbol{\theta}}}_q - \bar{\boldsymbol{\theta}}_r^{\mathrm{T}}\gamma_{wr}^{-1}\dot{\hat{\boldsymbol{\theta}}}_r - \bar{\eta}_u\gamma_{\eta u}^{-1}\dot{\hat{\eta}}_u - \bar{\eta}_q\gamma_{\eta q}^{-1}\dot{\hat{\eta}}_q - \bar{\eta}_r\gamma_{\eta r}^{-1}\dot{\hat{\eta}}_r\,.
\end{aligned} \tag{41}$$

Then, we define the following system robust terms:

$$\psi_{bs}=\mathbf{g}^{\mathrm{T}}(\bar{\psi})\mathbf{M}^{\mathrm{T}}\begin{bmatrix}\chi_\xi\\ \chi_\eta\\ \chi_\varsigma\end{bmatrix}u_r,\ \theta_{bs}=\mathbf{g}^{\mathrm{T}}(\bar{\theta})\mathbf{N}^{\mathrm{T}}\begin{bmatrix}\chi_\xi\\ \chi_\eta\\ \chi_\varsigma\end{bmatrix}u_r \tag{42}$$

$$u_{bs}=\mathbf{E}^{\mathrm{T}}\begin{bmatrix}\chi_\xi\\ \chi_\eta\\ \chi_\varsigma\end{bmatrix},\ r_{bs}=\frac{\chi_\psi}{\cos\theta},\ q_{bs}=\chi_\theta\ . \tag{43}$$

Substituting Eqs. (42) and (43) into Eq. (41) yields:

$$\begin{aligned}\dot{E}_3&=-\alpha_\xi\chi_\xi^2-\alpha_\eta\chi_\eta^2-\alpha_\varsigma\chi_\varsigma^2-\alpha_\psi\chi_\psi^2-\alpha_\theta\chi_\theta^2-\alpha_u\bar{u}^2-\alpha_q\bar{q}^2\\&-\alpha_r\bar{r}^2-\chi_u\left(\bar{\boldsymbol{\theta}}_u\boldsymbol{\xi}(\mathbf{x}_u)+\hat{\eta}_u\tanh(\nu\hat{\eta}_u\bar{u}\mu_u^{-1})+\varepsilon_u+\tau_{eu}(t)\right)\\&-\chi_q\left(\bar{\boldsymbol{\theta}}_q\boldsymbol{\xi}(\mathbf{x}_q)+\hat{\eta}_q\tanh(\nu\hat{\eta}_q\bar{q}\mu_q^{-1})+\varepsilon_q+\tau_{eq}(t)\right)\\&-\chi_r\left(\bar{\boldsymbol{\theta}}_r\boldsymbol{\xi}(\mathbf{x}_r)+\hat{\eta}_r\tanh(\nu\hat{\eta}_r\bar{r}\mu_r^{-1})+\varepsilon_r+\tau_{er}(t)\right)\\&-\bar{\boldsymbol{\theta}}_u^{\mathrm{T}}\gamma_{wu}^{-1}\dot{\hat{\boldsymbol{\theta}}}_u-\bar{\boldsymbol{\theta}}_q^{\mathrm{T}}\gamma_{wq}^{-1}\dot{\hat{\boldsymbol{\theta}}}_q-\bar{\boldsymbol{\theta}}_r^{\mathrm{T}}\gamma_{wr}^{-1}\dot{\hat{\boldsymbol{\theta}}}_r-\bar{\eta}_u\gamma_{\eta u}^{-1}\dot{\hat{\eta}}_u\\&-\bar{\eta}_q\gamma_{\eta q}^{-1}\dot{\hat{\eta}}_q-\bar{\eta}_r\gamma_{\eta r}^{-1}\dot{\hat{\eta}}_r\ .\end{aligned} \tag{44}$$

Then, Eq. (44) can be expressed by considering the Lemma in Ref. [32]: The inequality $h|x|\le xh\tanh(\nu hx/\mu_t)+\mu_t$ is true for all $\mu_t>0$, and $\forall x\in\Re,\forall h\in\Re$, where $\nu=e^{-(\nu+1)}$, $\nu=0.2785$. $\bar{\boldsymbol{\theta}}_k^{\mathrm{T}}\hat{\boldsymbol{\theta}}_k\le -c_1\left\|\bar{\boldsymbol{\theta}}_k\right\|_F^2+c_2\left\|\boldsymbol{\theta}_k^*\right\|_F^2,\tilde{\eta}_k(\hat{\eta}_k-\eta_{k0})\le -c_1\left|\tilde{\eta}_k\right|^2+c_2\left|\eta_k^*-\eta_{k0}\right|^2$, $\left|\tau_{ek}(t)+\varepsilon_k\right|\le\eta_k, k=u,q,r$,where $c_1=1-0.5\alpha^2$ and $c_2=0.5\alpha^2$ and $\alpha>\sqrt{2}/2$, and then combining Eqs. (30), (32) and (34):

$$\begin{aligned}\dot{E}_3&\le-\alpha_\xi\chi_\xi^2-\alpha_\eta\chi_\eta^2-\alpha_\varsigma\chi_\varsigma^2-\alpha_\psi\chi_\psi^2-\alpha_\theta\chi_\theta^2-\alpha_u\bar{u}^2-\alpha_q\bar{q}^2\\&-\alpha_r\bar{r}^2-c_1\lambda_u\left\|\bar{\boldsymbol{\theta}}_u\right\|_F^2-c_1\lambda_q\left\|\bar{\boldsymbol{\theta}}_q\right\|_F^2-c_1\lambda_r\left\|\bar{\boldsymbol{\theta}}_r\right\|_F^2-c_1\kappa_u\left|\bar{\eta}_u\right|^2\\&-c_1\kappa_q\left|\bar{\eta}_q\right|^2-c_1\kappa_r\left|\bar{\eta}_r\right|^2+c_2\lambda_u\left\|\boldsymbol{\theta}_u^*\right\|_F^2+c_2\lambda_q\left\|\boldsymbol{\theta}_q^*\right\|_F^2\\&+c_2\lambda_r\left\|\boldsymbol{\theta}_r^*\right\|_F^2+c_2\kappa_u\left|\eta_u^*-\eta_{u0}\right|^2+c_2\kappa_q\left|\eta_q^*-\eta_{q0}\right|^2\\&+c_2\kappa_r\left|\eta_r^*-\eta_{r0}\right|^2+\mu_u+\mu_q+\mu_r\ .\end{aligned} \tag{45}$$

Now, Eq. (45) gives as

$$\dot{E}_3(t)\le-(\lambda_{\mathrm{m}}/\lambda_{\mathrm{x\,max}})E_3(t)+\mu \tag{46}$$

where $\lambda_{\mathrm{m}}=\min\{\alpha_\xi,\alpha_\eta,\alpha_\varsigma,\alpha_\psi,\alpha_\theta,\alpha_u,\alpha_q,\alpha_r,c_1\lambda_u,c_1\lambda_q,c_1\lambda_r,c_1\kappa_u,$ $c_1\kappa_q,c_1\kappa_r\}$; $\lambda_{\mathrm{x\,max}}=\max\{1,m_{11},m_{55},m_{66},\lambda_{wu}^{-1},\lambda_{wq}^{-1},\lambda_{wr}^{-1},\lambda_{\eta u}^{-1},\lambda_{\eta q}^{-1},\lambda_{\eta r}^{-1}\}$, and:

$$\begin{aligned}\mu&=c_2\lambda_u\left\|\boldsymbol{\theta}_u^*\right\|_F^2+c_2\lambda_q\left\|\boldsymbol{\theta}_q^*\right\|_F^2+c_2\lambda_r\left\|\boldsymbol{\theta}_r^*\right\|_F^2+c_2\kappa_u\left|\eta_u^*-\eta_{u0}\right|^2\\&+c_2\kappa_q\left|\eta_q^*-\eta_{q0}\right|^2+c_2\kappa_r\left|\eta_r^*-\eta_{r0}\right|^2+\mu_u+\mu_q+\mu_r\ .\end{aligned} \tag{47}$$

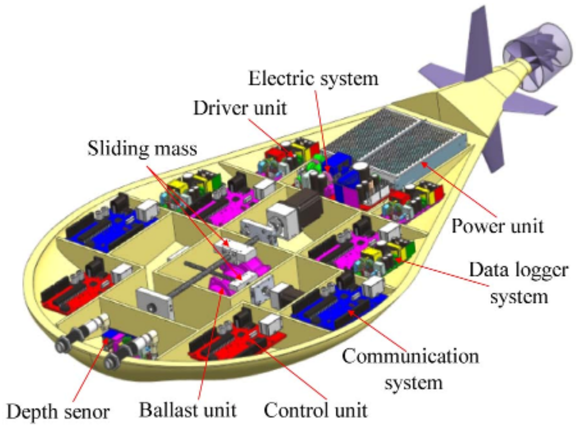

Fig. 5. The underactuated flying-wing AUV structure.

Thus, it could be concluded that all of the signals in the overall proposed control strategy are uniformly ultimately bounded. In addition, the errors in the path following control structure exponentially tend to a narrow region near the zero. Thus, the proof is completed.

5. Simulation and comparative analysis

In this section, the robust performance and efficiency of the proposed path following control structure are investigated. All of simulations are implemented through MATLAB software environment. The simulations are performed on an underactuated flying-wing AUV established by Harbin Institute of Technology in China that is shown in Fig. 5. The flying-wing AUV parameters are shown in Ref. [33].

Consider that the AUV in the mission should follow the following curvilinear path:

$$\begin{cases}x_d(\varpi)=20\cos\left(\dfrac{\pi}{26}\varpi\right)+10\\ y_d(\varpi)=20\sin\left(\dfrac{\pi}{26}\varpi\right)+5\\ z_d(\varpi)=-\varpi-5\ .\end{cases} \tag{48}$$

The initial conditions of the underactuated AUV are given by $x(0)=10m,y(0)=0m,z(0)=0m,\theta(0)=0^\circ,\psi(0)=40^\circ$, and initial velocities are $u(0)=0m/s,v(0)=0m/s,w(0)=0m/s$, and the virtual reference velocity can be considered as $u_r=u_0\left(1-\tanh\left(\xi/\delta\right)\right)$,where $u_0=1m/s$ and $\delta=0.5$.

To evaluate the efficiency and robust performance of the proposed controller in the complex ocean environment, we assume that the parameters of the AUV are unknown completely and the AUV is influenced by the external disturbances as follows:

$$\mathbf{d}(t)+\mathbf{T}\dot{\mathbf{d}}(t)=\mathbf{K}\omega_0 \tag{49}$$

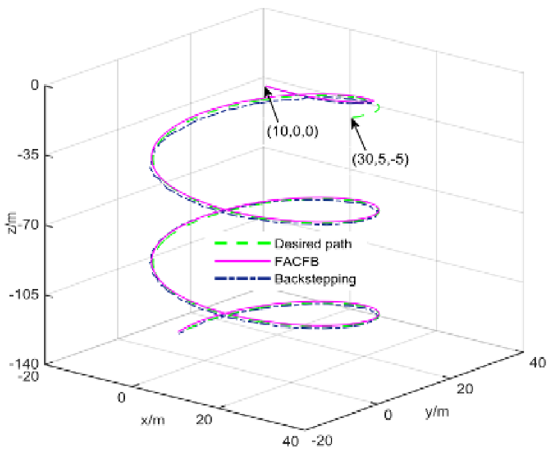

Fig. 6. Path following trajectory of the underactuated AUV.

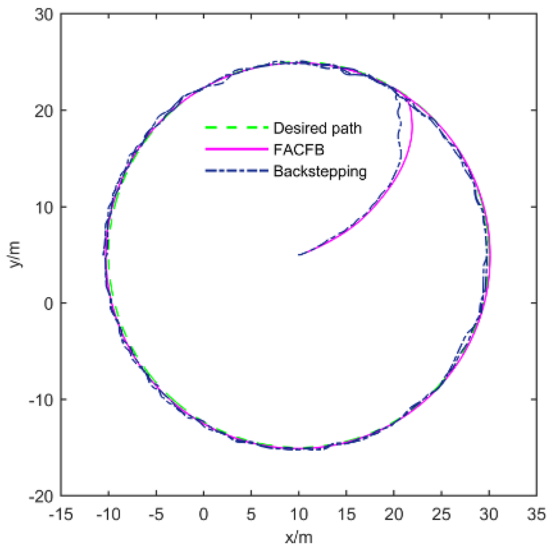

Fig. 7. Horizontal projection of the following trajectory of AUV.

where $\mathbf{d}(t)=[\tau_{eu}(t),\tau_{ev}(t),\tau_{ew}(t),\tau_{eq}(t),\tau_{er}(t)]^{\mathrm{T}}$,and ω_0 denotes the white noise disturbance. $\mathbf{K}=diag\{8,5,5,8,8\}$ is the gain parameter matrix, and $\mathbf{T}=diag\{5,5,5,5,5\}$ represents the time constant matrix.

In this simulation, the controller gains are set to $\alpha_\xi=15$, $\alpha_\eta=8$, $\alpha_\zeta=6$, $\alpha_\psi=\alpha_\theta=8$, $\alpha_u=20$, $\alpha_q=\alpha_r=10$, $\gamma_{wu}=20$, $\gamma_{wq}=16$, $\gamma_{wr}=12$, $\lambda_u=0.2$, $\lambda_q=0.1$, $\lambda_r=0.15$, $\gamma_{\eta u}=4$, $\gamma_{\eta q}=2$, $\gamma_{\eta r}=2$, $\kappa_u=0.2$, $\kappa_q=0.1$, $\kappa_r=0.05$, $\rho_1=1$, $\sigma_1=0.25$, $\rho_2=2\pi/3$, $\sigma_2=\pi/12$, $\rho_3=\pi/3$, $\sigma_3=\pi/12$ and the parameters of second-order filter are given by $\omega_n=20\text{ rad/s}$ and $\upsilon=0.9$.

The simulation results based on the fuzzy adaptive command filtered backstepping (FACFB) and the traditional backstepping approach which is proposed in Ref. [34] are shown in Figs. 6-12.

The simulation results given in Figs. 6-8 demonstrate that the proposed controller scheme leads to the AUV 3D path following under considerable multiple uncertainties and the measurement noise. As could be seen from Fig. 9, the proposed control scheme has more excellent accuracy of path

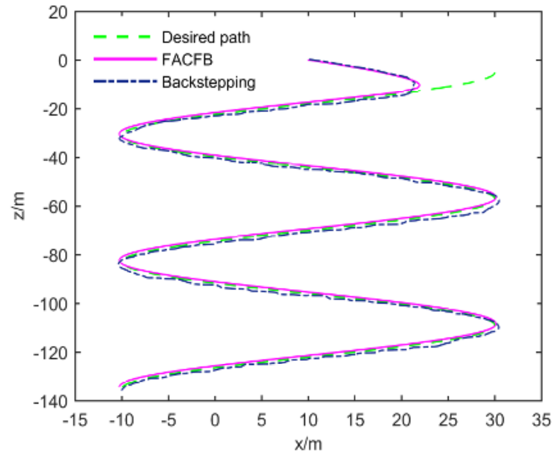

Fig. 8. Vertical projection of the following trajectory of AUV.

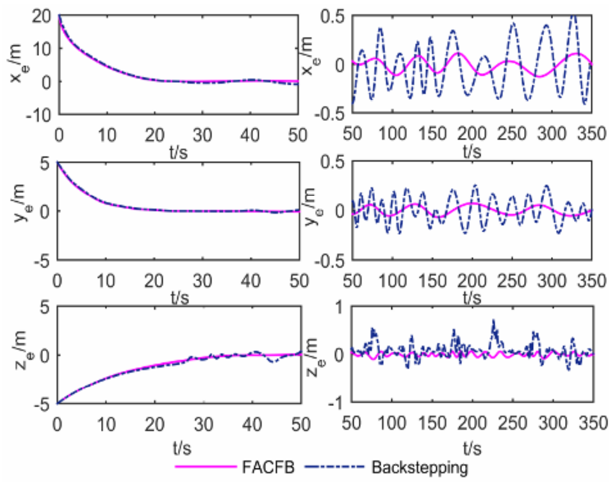

Fig. 9. Path following errors of the flying-wing AUV.

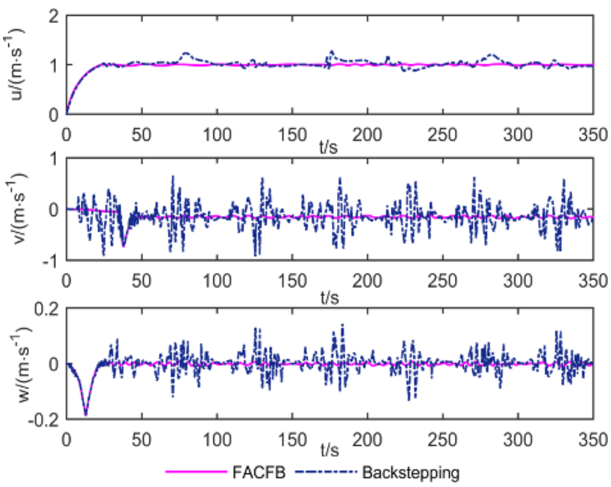

Fig. 10. Velocity responses of the underactuated AUV.

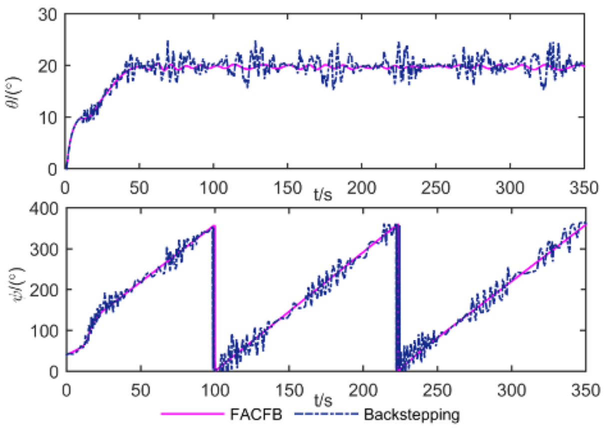

Fig. 11. Angle responses of the underactuated AUV.

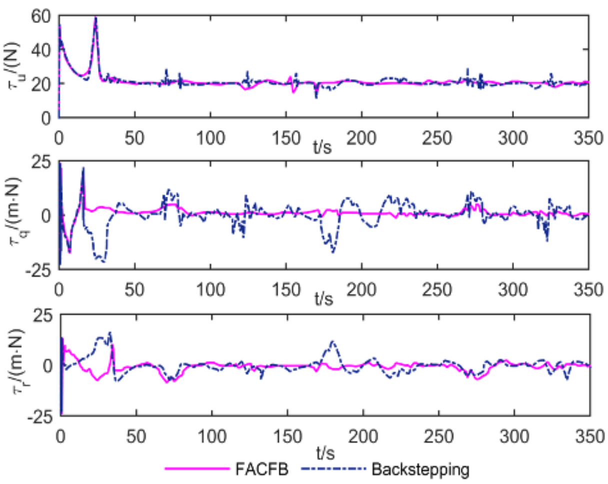

Fig. 12. Control forces and moments of the underactuated AUV.

following compared with traditional backstepping approach.

As shown in Figs. 10 and 11, the proposed control structure is robust to the parameter uncertainties and external disturbances compared with the traditional backstepping method. This demonstrates that superior robust performance could be obtained via the proposed controller. Finally, the control inputs of controllers are shown in Fig. 12.

6. Conclusion

The 3D path following control problem for the underactuated AUV subject to parameter uncertainties and external disturbances is verified in this paper. With the error model of the 3D path following established based on the virtual guidance method, a fuzzy-adaptive command filtered backstepping controller is developed, which can not only restrain the multiple uncertainties as well as external disturbances, but also decrease the computational effort of standard backstepping method. Simulation results indicate that the proposed 3D path following control structure could provide higher path following precision as well as superior robustness compared with the traditional backstepping controller. Finally, it should be pointed out that the experimental verifications are not carried out due to the limitation of the conditions. As a future study, the performance of the proposed method could be investigated through experimental tests.

Acknowledgment

The authors acknowledge support by the National Natural Science Foundation of China (NSFC, Grant Nos. 11672094).

References

[1] M. L. Corradini and G. Orlando, Robust quantized feedback stabilization of linear systems, *Automatica*, 44 (9) (2008) 2458-2462.
[2] P. Batista, C. Silvestre and P. Oliviera, A sensor-based controller for homing of underactuated AUVs, *IEEE Transactions on Robotics*, 25 (3) (2009) 701-716.
[3] S. Campbell, W. Naeem and G. W. Irwin, A review on improving the autonomy of unmanned surface vehicles through intelligent collision avoidance manoeuvres, *Annual Reviews in Control*, 36 (2) (2012) 267-283.
[4] R. B. Wynn and V. A. Huvenne, Autonomous underwater vehicles (AUVs): Their past, present and future contributions to the advancement of marine geoscience, *Marine Geology*, 352 (1) (2014) 451-468.
[5] Y. Shi, C. Shen, H. Z. Fang and H. P. Li, Advanced control in marine mechatronic systems: A survey, *IEEE/ASME Trans. Mechatronics*, 22 (3) (2017) 1121-1131.
[6] M. Bibuli, A. Pascoal and P. Ridao, Introduction to the special section on navigation, control, and sensing in the marine environment, *Annual Reviews in Control*, 40 (2015) 127-128.
[7] K. Y. Wichlund, O. J. Sordalen and O. Egeland, Control properties of underactuated vehicles, *Proc. of IEEE Internat-ional Conference on Robotics and Automation*, IEEE (1995) 2009-2014.
[8] J. Garus and B. Zak, Using of soft computing techniques to control of underwater robot, *Proc. of International Conference on Methods and Models in Automation and Robotics*, IEEE (2010) 415-419.
[9] E. Borhaug, A. Pavlov and K. Y. Pettersen, Integral LOS control for path following of underactuated marine surface vessels in the presence of constant ocean currents, *Proc. of the 47th IEEE Conference Decision and Control*, IEEE (2008) 4984-4991.
[10] A. M. Lekkas and T. I. Fossen, Integral LOS path following for curved paths based on a monotone cubic Hermite spline parametrization, *IEEE Transactions on Control Systems Technology*, 22 (6) (2014) 2287-2301.
[11] Z. W. Zheng, L. Sun and L. H. Xie, Error-constrained LOS path following of a surface vessel with actuator saturation and faults, *IEEE Transactions on Systems, man, and*

Cybern-etics: Systems, 48 (10) (2018) 1794-1805.
[12] F. Repoulias and E. Papadopoulos, Planar trajectory planning and tracking control design for underactuated AUVs, *Ocean Engineering*, 34 (11) (2007) 1650-1667.
[13] M. Roozegar, M. J. Mahjoob and M. Ayati, Adaptive tracking control of a nonholonomic pendulum-driven spherical robot by using a model-reference adaptive system, *Journal of Mechanical Science and Technology*, 32 (2) (2018) 845-853.
[14] X. Liang, X. J. Hua, L. F. Su, W. Li and J. D. Zhang, Path following control for underactuated AUV based on feedback gain backstepping, *Technical Gazette*, 22 (4) (2015) 829-835.
[15] J. Gao, W. S. Yan, N. N. Zhao and D. M. Xu, Global path following control for unmanned underwater vehicles, *Proc. of the 29th Chinese Control Conference*, IEEE (2010) 3188-3192.
[16] L. Liu, D. Wang and Z. Peng, Coordinated path following of multiple underacutated marine surface vehicles along one curve, *Isa Transactions*, 64 (2016) 258-268.
[17] Z. H. Peng, D. Wang, Z. Y. Chen and X. J. Hu, Adaptive dynamic surface control for formations of autonomous surface vehicles with uncertain dynamics, *IEEE Transactions on Control Systems Technology*, 21 (2) (2013) 513-520.
[18] Z. Zheng and L. Sun, Path following control for marine surface vessel with uncertainties and input saturation, *Neurocomputing*, 177 (2016) 158-167.
[19] J. Lorentz and J. Yuh, A survey and experimental study of neural network AUV control, *Proc. of Autonomous Under-water Vehicle Technology*, IEEE (1996) 109-116.
[20] X. B. Xiang, C. Yu and Q. Zhang, Robust fuzzy 3D path following for autonomous underwater vehicle subject to uncertainties, *Computers and Operations Research*, 84 (2016) 165-177.
[21] J. Guo, F. C. Chiu and C. C. Huang, Design of a sliding mode fuzzy controller for the guidance and control of an autonomous underwater vehicle, *Ocean Engineering*, 30 (16) (2003) 2137-2155.
[22] X. Liang, L. Wan and J. I. R. Blake, Path following of an underactuated AUV based on fuzzy backstepping sliding mode control, *International Journal of Advanced Robotic Systems*, 13 (3) (2016) 1-11.
[23] N. Wang and J. E. Meng, Direct adaptive fuzzy tracking control of marine vehicles with fully unknown parametric dynamics and uncertainties, *IEEE Transactions on Control Systems Technology*, 24 (5) (2016) 1845-1852.
[24] K. D. Do, J. Pan and Z. P. Jiang, Robust and adaptive path following for underactuated autonomous underwater vehicles, *Ocean Engineering*, 31 (16) (2004) 1967-1997.
[25] X. Qi, Spatial target path following control based on Nussbaum gain method for underactuated underwater vehicle, *Ocean Engineering*, 104 (2015) 680-685.
[26] H. J. Wang, Z. Y. Chen and J. H. Jia, Underactuated AUV 3D path tracking control based filter backstepping method, *Acta Automatica Sinica*, 41 (3) (2015) 631-645.
[27] K. D. Do, Coordination control of underactuated ODINs in three-dimensional space, *Robotics and Autonomous Systems*, 61 (8) (2013) 853-867.
[28] K. Y. Pettersen and O. Egeland, Time-varying exponential stabilization of the position and attitude of an underactuated autonomous underwater vehicle, *IEEE Transactions on Automatic Control*, 44 (1) (1999) 112-115.
[29] J. M. Miao, S. P. Wang, Z. P. Zhao, Y. Li and M. M. Tomovic, Spatial curvilinear path following control of underactuated AUV with multiple uncertainties, *ISA Transactions*, 67 (2017) 107-130.
[30] M. Breivik and T. I. Fossen, Principles of guidance-based path following in 2D and 3D, *Proc. of the 44th IEEE Conference on Decision and Control*, IEEE (2005) 627-634.
[31] F. Y. Bi, J. Z. Zhang and Y. J. Wei, Robust position tracking control design for underactuated AUVs, *Journal of Harbin Institute of Technology*, 42 (11) (2010) 1690-1695.
[32] M. M. Polycarpou, Stable adaptive neural control scheme for nonlinear system, *IEEE Transactions on Automatic Control*, 41 (3) (2002) 447-451.
[33] J. Q. Wang, C. Wang and Y. J. Wei, Hydrodynamic characteristics and motion simulation of flying-wing dish-shaped autonomous underwater glider, *Harbin Institute of Technology*, 50 (4) (2018) 131-137.
[34] Y. T. Wang, W. S. Yan, B. Gao and R. X. Cui, Backstepping-based path following control of an underactuated autonomous underwater vehicle, *Proc. of International Conference on Information and Automation*, IEEE (2009) 466-471.

JinQiang Wang was born in Harbin, Heilongjiang Province, China. He received the B.E. degree in naval architecture and ocean engineering from the School of Shipbuilding Engineering, Harbin Engineering University, Harbin, China, in 2016. He is now pursuing his Ph.D. degree in astronautics at Harbin Institute of Technology. His current research interests include guidance and the motion control of autonomous underwater vehicles.

Cong Wang received his Ph.D. degree in mechanics from Harbin Institute of Technology, Harbin, China, in 2001. He received his Bachelor and Master degrees in mechanical and electrical engineering from Northeast Forestry University in 1989 and 1993, respectively. He is currently a Professor at School of Astronautics, Harbin Institute of Technology, China. His current research interests include fluid mechanics and the motion control of underwater vehicles.

YingJie Wei received his Ph.D. degree in mechanics from Harbin Institute of Technology, Harbin, China, in 2003. He received his bachelor and master degrees in oil and gas field development from the Northeast Petroleum University in 1996 and 2000, respectively. He is currently a Professor at School of Astronautics, Harbin Institute of Technology, China. His current research interests include multiphase fluid mechanics and hydrodynamics of the underwater vehicles.

ChengJu Zhang received the B.E. degree in naval architecture and ocean engineering from the School of Shipbuilding Engineering, Harbin Engineering University, Harbin, China, in 2017. He is now pursuing his Ph.D. degree in astronautics at Harbin Institute of Technology. His current research interests include the motion control of marine surface vehicles.